Monatsh Chem (2011) 142:421–430
DOI 10.1007/s00706-011-0470-1

ORIGINAL PAPER

Beta-amyloid toxicity increases with hydrophobicity in the presence of metal ions

Alberto Granzotto · Silvia Bolognin · Janez Scancar · Radmila Milacic · Paolo Zatta

Received: 9 September 2010 / Accepted: 21 February 2011 / Published online: 24 March 2011

Abstract Alzheimer's disease is a multifactorial neurodegenerative disorder characterized by the pathological brain deposition of neurofibrillary tangles and senile plaques. The latter consist mainly of insoluble β-amyloid (Aβ) fibril deposition. Aβ aggregation and deposition can be increased by several factors, including metal ions. In this study we investigated the role played by metal ions in affecting Aβ oligomerization in the presence and in the absence of its hydrophobic fragment A$\beta_{17–28}$. This was done not as a physiological investigation, but as a paradigmatic study to confirm the key role of Aβ superficial hydrophobicity as a relevant aggravating factor that contributes to the toxicity of Aβ and Aβ–metal complexes. The structural conformations of Aβ–metal complexes were monitored through fluorescence and turbidity measurements as well as transmission electron microscopy. Results reported herein indicate that various metals differentially influence Aβ conformation, with aluminum being the only metal ion for which we are able to determine a dramatic enhancement of peptide oligomer formation with a consequent toxic effect. This scenario was further enhanced by the presence of A$\beta_{17–28}$, which resulted in a marked toxicity in a neuroblastoma cell culture as a consequence of the enhancement of the hydrophobicity of the amyloid and amyloid–metal complexes.

A. Granzotto · S. Bolognin · P. Zatta (✉)
Department of Biology, Padua "Metalloproteins" Unit, CNR-Institute for Biomedical Technologies, University of Padua, Padua, Italy
e-mail: zatta@bio.unipd.it

J. Scancar · R. Milacic
Department of Environmental Sciences, Josef Stefan Institute, Ljubljana, Slovenia

Keywords Amyloid-beta · Aluminum · Alzheimer's disease · Metal ions · Hydrophobicity

Introduction

Even though more than 100 years have passed since Alzheimer's disease (AD) was first described, there are still no satisfactory explanations for the conditions that lead to the primum movens and the consequent development of the disease. Although the multifactorial character of the disease makes it difficult to identify the potential etiopathogenetic contributory factors, histologically AD is characterized by the loss of neuronal density in the cerebral cortex, the presence of intraneuronal neurofibrillary tangles (NFTs) consisting of hyperphosphorylated tau proteins (τ) [1], and senile plaques (SPs) formed by the extraneuronal deposition of β-amyloid protein (Aβ). Aβ is a byproduct of the metabolism of a transmembrane precursor (AβPP), and it is cleaved by two proteolytic enzymes called β- and γ-secretase. Recent studies have proposed that Aβ follows a complex process of oligomerization/aggregation. This starts with the formation of monomers, followed by soluble, low molecular weight (LMW) oligomeric structures that exhibit an increase in β-sheet content [2]. Oligomers associate rapidly to form higher-order insoluble aggregates called fibrils. Fibrils are the main constituent of SPs, although the presence of SPs is not necessarily an indication of AD. Recent evidence underlines a strong association between histological features of AD and dementia in patients in their mid-70s [3]. Nevertheless, many authors identify the important role played by soluble Aβ oligomers in the initial steps of AD, due to the oligomers' potent synaptotoxicity [4]. The progression of Aβ aggregation is influenced by many factors, including the presence of metal ions; many studies suggest that

endogenous biometals such as copper, zinc and iron as well as exogenous biometals such as aluminum play a potential role in Aβ aggregation and bio-availability [5]. Accordingly, several reports have demonstrated a marked accumulation of metal ions in the SP and in the neurophils of AD patients [6, 7]; this evidence has been also quantitatively confirmed by Leskovjan et al. [8] for copper, iron, and zinc. The Aβ aggregation model is further complicated by other variables, such as Aβ_{1-42} hydrophobicity. Meanwhile, although the role of lipophilicity in promoting Aβ_{1-42} aggregation [9, 10] seems to be clear, the importance of Aβ_{1-42} surface hydrophobicity as a possible mechanism of toxicity has not been sufficiently investigated. With this experimental model, carried out using a nonphysiological Aβ_{1-42} truncated fragment as a hydrophobicity enhancer, we would like to stress the importance of lipophilicity in promoting Aβ_{1-42} toxicity, mainly in the presence of metal ions.

Results and discussion

Fluorescence

Thioflavin T (ThT) is known to rapidly bind the β-sheet-rich aggregated form of peptides. ThT fluorescence over time for samples of Aβ_{1-42}, Aβ_{1-42}–metal complexes and Aβ_{17-28} were examined.

A lag time prior to the formation of β-sheet structures which occurs after $\sim$5 h for both Aβ_{17-28} and Aβ_{17-28} + Fe was observed. The aggregation was enhanced in the presence of the other metals tested. Al is the metal that most affects the process. The absence of a lag time in the sample Aβ_{17-28} + Al may suggest the possibility of an immediate conversion of monomeric Aβ_{17-28} into ThT-reactive species, such as oligomers [14] and protofibrils [15].

Then we used ThT to follow changes in β-sheet content in samples of Aβ_{1-42}/Aβ_{1-42}–metal complexes to which Aβ_{17-28} was initially added.

As shown in Fig. 1, the fluorescence of Aβ_{1-42} + Aβ_{17-28} increased in a sigmoidal manner, indicating the formation of aggregating structures. This curve is consistent with a nucleation-dependent model [16]. The nucleation phase was skipped and the elongation phase emerged rapidly as soon as the two peptides interacted with each other. This general trend is not observed for either Aβ_{1-42}–Fe + Aβ_{17-28} or for Aβ_{1-42}–Cu + Aβ_{17-28}. A marked increase in ThT fluorescence was observed in Aβ_{1-42}–Al + Aβ_{17-28} compared with Aβ_{1-42}–Al alone, suggesting that the interaction between the oligomers of the metal complex was involved in promoting nucleation assembly. The fact that Aβ_{1-42}–Zn precipitated indicates that the equilibrium of the protein species is shifted toward the formation of amorphous aggregates. The mechanism

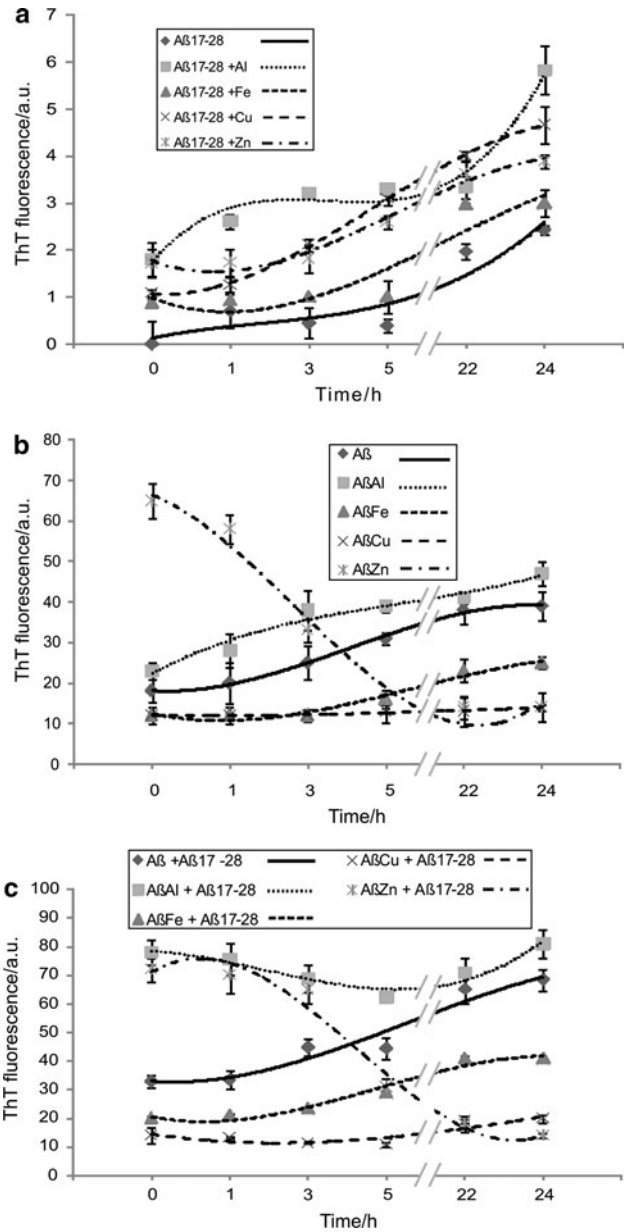

Fig. 1 Time dependence of the fluorescence emission intensity of ThT bound to Aβ_{17-28} both in the absence and in the presence of Al, Cu, Fe, and Zn at a concentration of 5 μM (**a**), to Aβ_{1-42}–metal complexes (**b**), and to Aβ_{17-28} in the presence of Aβ_{1-42}–metal complexes **c**). The Aβ_{17-28}, Aβ_{1-42}, and Aβ_{1-42}–metal complex peptide concentrations were 5 μM. ThT (20 μM) fluorescence at 482 nm (λ_{exc} = 450 nm) was followed for 24 h. The emissions due to the free dye and buffer were subtracted. The data represented are the mean ± SD of three individual experiments

was not reversible, since mixing the solution did not re-suspend the aggregate. All samples (except Aβ_{1-42}–Zn + Aβ_{17-28}) showed a sigmoidal curve characterized by a $\sim$3/5 h lag time, followed by a $\sim$19 h period where ThT fluorescence increased. After 24 h of incubation at room temperature a plateau was observed.

$A\beta_{1-42}$ + $A\beta_{17-28}$, $A\beta_{1-42}$–Al + $A\beta_{17-28}$, $A\beta_{1-42}$–Fe + $A\beta_{17-28}$, $A\beta_{1-42}$–Cu + $A\beta_{17-28}$, and $A\beta_{1-42}$–Zn + $A\beta_{17-28}$ were each tested for surface hydrophobicity by following the 8-anilino-1-naphthalene sulfonic acid (ANS) probe. According to Uversky et al. [17], changes in ANS fluorescence (an increase in intensity and a blue shift of the emission maximum) are characteristic of the interaction of this dye with the solvent-exposed hydrophobic clusters of partially folded peptides and proteins.

Figure 2 shows that $A\beta_{1-42}$–Al induced an increase in ANS fluorescence intensity and a blue shift of the emission maximum compared with the other Aβ–metal complexes. This implies that the peptide is converted into a more folded conformation with solvent-exposed hydrophobic clusters. This conversion was higher in the presence of $A\beta_{1-42}$–Al + $A\beta_{17-28}$.

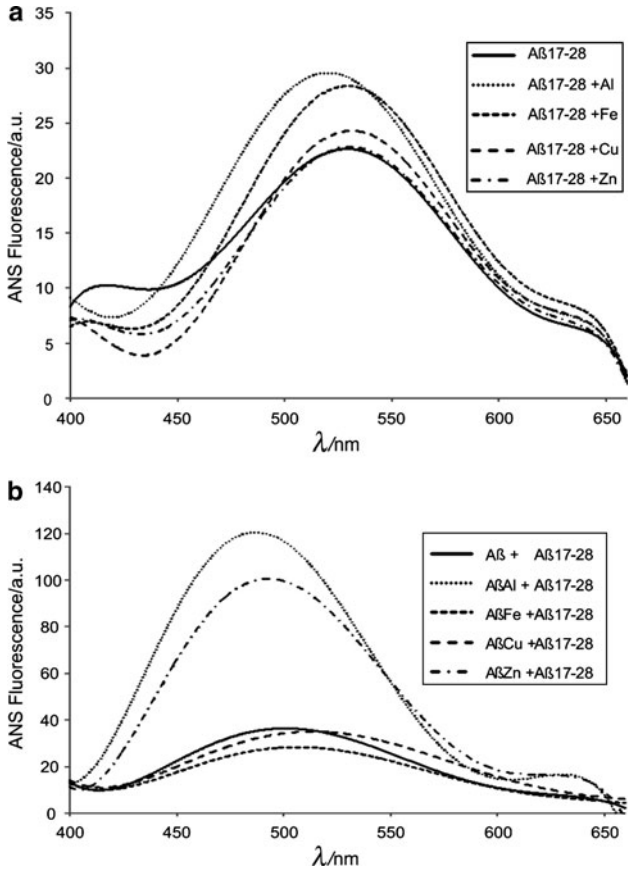

Fig. 2 Fluorescence emission spectra of ANS (25 μM) after interaction with $A\beta_{17-28}$ both in the absence and in the presence of Al, Cu, Fe, and Zn at a concentration of 5 μM (**a**), and with $A\beta_{17-28}$ in the presence of $A\beta_{1-42}$–metal complexes (**b**). Emission spectra were recorded from 400 to 700 nm with excitation at 360 nm. The [$A\beta_{17-28}$]/[$A\beta_{1-42}$] ratio was equal to 1. The signals due to the free dye and buffer were subtracted. The peptide samples (5 μM) were left to incubate for 24 h at room temperature, and then the fluorescence was measured

Surprisingly, $A\beta_{1-42}$–Zn in the presence of $A\beta_{17-28}$ decreased its propensity to expose hydrophobic clusters. Simultaneously, we did not observe any significant difference in ANS fluorescence with $A\beta_{1-42}$–Fe, $A\beta_{1-42}$–Cu, and $A\beta_{1-42}$ alone in the presence of the $A\beta_{1-42}$ truncated fragment. In our opinion, these more hydrophobic complexes can be considered a good model for studying the effects of hydrophobicity in relation to $A\beta_{1-42}$–metal complex toxicity. In fact, lipophilicity could play a crucial role in increasing the deleterious effects of $A\beta_{1-42}$–metal complexes.

Turbidity

To clarify the effect of $A\beta_{17-28}$ on $A\beta_{1-42}$/$A\beta_{1-42}$–metal complex fibrillization, aggregation was also assayed by measuring the turbidity at 405 nm wavelength. A turbidity assay gives information on the quantity but not the quality of the aggregates.

First of all, the capacity of $A\beta_{17-28}$ to create complexes with metal ions was tested. When Al was present, there was a dramatic increase in the $A\beta_{17-28}$ aggregation rate which stabilized after 24 h of incubation. The other metals (Fe, Cu, and Zn) exerted only negligible effects. Stabilization of the aggregation process was observed after 24 h of incubation.

As for the role played by $A\beta_{17-28}$ in solution with $A\beta_{1-42}$–metal complexes, as suggested by ThT fluorescent assay, the presence of $A\beta_{17-28}$ stimulated aggregate formation in the $A\beta_{1-42}$–Al samples while the other conditions were not affected, especially when compared with $A\beta_{1-42}$–Al + $A\beta_{17-28}$. For $A\beta_{17-28}$, we observed a plateau in the aggregation process after 24 h, which was also seen for $A\beta_{1-42}$–metal complexes.

Transmission electron microscopy

To assess the morphology of aggregates formed in the presence of $A\beta_{17-28}$, the peptide fragment was incubated with $A\beta_{1-42}$ and $A\beta_{1-42}$–metal complexes. Aliquots were removed at time zero and after 24 h of incubation at room temperature. In the presence of $A\beta_{1-42}$–Al + $A\beta_{17-28}$, we observed small spherical oligomers resembling those previously reported in the presence of $A\beta_{1-42}$–Al alone by Drago et al. [18].

After 24 h of incubation, the presence of $A\beta_{17-28}$ stimulated the formation of protofibrillar structures that could not be detected in the presence of $A\beta_{1-42}$–Al alone (data not shown). These spherical oligomers contained an extended β-sheet structure, as detected by ThT fluorescence. $A\beta_{1-42}$–Cu + $A\beta_{17-28}$ showed minimal aggregation at time zero but started to aggregate into well-structured fibrils after 24 h. $A\beta_{1-42}$–Fe + $A\beta_{17-28}$ appeared to form small fibrils together with amorphous aggregates at time zero; then, after 24 h, fibrils became the dominant

species. These fibrils often formed large groups containing randomly oriented fibers. At time zero, the samples $A\beta_{1-42}$ + $A\beta_{17-28}$ showed minimal aggregation, consistent with the majority of $A\beta$ being in nonaggregated form. A significant increase in the rate of aggregation was observed after 24 h and this correlated with the increase in ThT fluorescence. $A\beta_{1-42}$–Zn + $A\beta_{17-28}$ showed no aggregation at time zero but a longer incubation period (24 h) resulted in the appearance of fibrils, which seemed to coexist with oligomers. Taken together, TEM images suggested that the presence of $A\beta_{17-28}$ enhanced $A\beta_{1-42}$ and $A\beta_{1-42}$–metal complex fibrillization, stimulating both fibril elongation and nucleation. When the peptide was present the type of aggregate formed seemed to be more regular, but in the case of $A\beta_{1-42}$–Al a lower rate of aggregation compared with the other treatments was still maintained after 24 h.

Toxicity to cell culture

We initially examined the concentration dependence of the toxicity of $A\beta_{17-28}$. SHSY5Y were treated with $A\beta_{17-28}$ in a range of concentrations between 0.01 and 5 μM.

The toxicity to SHSY5Y was evaluated by a standard MTT assay. We found that the fragment concentration that inhibits 50% (IC_{50}) of the cell viability was higher than 5 μM. The other concentrations tested showed no or minimal toxicity. The first nontoxic concentration was 0.1 μM. $A\beta_{17-28}$–metal complexes showed a negligible effect. We also tested the toxicity of metal ions alone (at a concentration of 5 μM) to exclude the possibility that the effects observed were due to the metal itself rather than the complex; we did not observe any toxicity.

Then, to establish a structure–activity relationship, we also determined the effect of $A\beta_{17-28}$–metal complexes (prepared by incubating $A\beta_{17-28}$ with a 50 μM solution of metal ions at a concentration ratio of 1:1). We had previously demonstrated [18] that the $A\beta_{1-42}$–Al complex is more effective at decreasing cell viability than $A\beta_{1-42}$ alone or the other $A\beta_{1-42}$–metal complexes. Here we showed that an interaction between $A\beta_{1-42}$–Al and $A\beta_{17-28}$ produced a new toxic species which was significantly more toxic not only when compared with the control but also when compared with $A\beta_{1-42}$–Al. Simultaneously, we observed that all the other treatments with $A\beta_{1-42}$–metals + $A\beta_{17-28}$ showed a modest increase in cell toxicity compared with $A\beta_{1-42}$–metal complexes alone. The latter statement holds true except for $A\beta_{1-42}$–Cu + $A\beta_{17-28}$; its toxicity was significantly lower when compared with $A\beta_{1-42}$–Cu alone.

Consistent with the MTT data, morphological changes resulted in a reduction in the cellular body, neuritis, and neuronal cell number. We can exclude the idea that the toxicity was due merely to the activation of apoptotic pathways, because after 24 h of treatment, caspases 3 and 6 were not activated (data not shown). This implies that $A\beta_{1-42}$ and its metal complexes use a different mechanism of toxicity.

Scanning electron microscopy

Scanning electron microscopy (SEM) can give us a qualitative idea of toxicity of the treatment. We thus consider SEM images to be complementary data to the data gained through MTT cell viability assay.

In agreement with the MTT assay, the treatment with $A\beta_{17-28}$ did not show any differences in cell morphology compared with the control, thus confirming that $A\beta_{17-28}$ alone is not toxic.

As stated by several authors [19–21], the toxicity of $A\beta_{1-42}$ could originate from bilayer disruption and cell leakage. This statement is qualitatively confirmed by Fig. 3.

The cell membrane appears deeply damaged, but not homogeneously. Cell leakage is more evident in cells treated with $A\beta_{1-42}$–Al + $A\beta_{17-28}$ and $A\beta_{1-42}$–Cu + $A\beta_{17-28}$, while we do not observe significant variations in the presence of the other complexes, which matches with the MTT data.

Discussion

Alzheimer's disease, as well as other neurodegenerative diseases, could be classified as "conformational disorders" in that they are all characterized by a conformational rearrangement of specific proteins to form insoluble aggregates that deposit in the tissues [22].

It has been previously demonstrated by this laboratory that the propensity of $A\beta$ to aggregate can increase in the presence of some metal ions, and this aggregation led to an increase of in vitro toxicity to neuroblastoma cell cultures, especially when bound to Al^{3+}, forming the complex $A\beta$–Al [23]. To further understand the intriguing interrelationship between $A\beta$ and metal ions, the interaction between $A\beta_{1-42}$ and the $A\beta_{17-28}$ truncated fragment was studied.

This $A\beta_{1-42}$ truncated fragment was chosen for several reasons: it contains one of the most lipophilic parts of the $A\beta_{1-42}$ amino acid sequence but is also not toxic at the concentrations used; it is not a physiological fragment that could be involved in biochemical pathways, and it has the ability to stimulate the exposure of hydrophobic clusters without significantly affecting $A\beta_{1-42}$ and $A\beta_{1-42}$–metal complex oligomerization and fibrillization processes (as demonstrated by ThT assay and TEM micrographs).

Since a direct correlation between $A\beta$ toxicity and hydrophobicity has been demonstrated [25], we investigated the role of one of the $A\beta$'s most hydrophobic sequences in influencing $A\beta$ and $A\beta$–metal complex

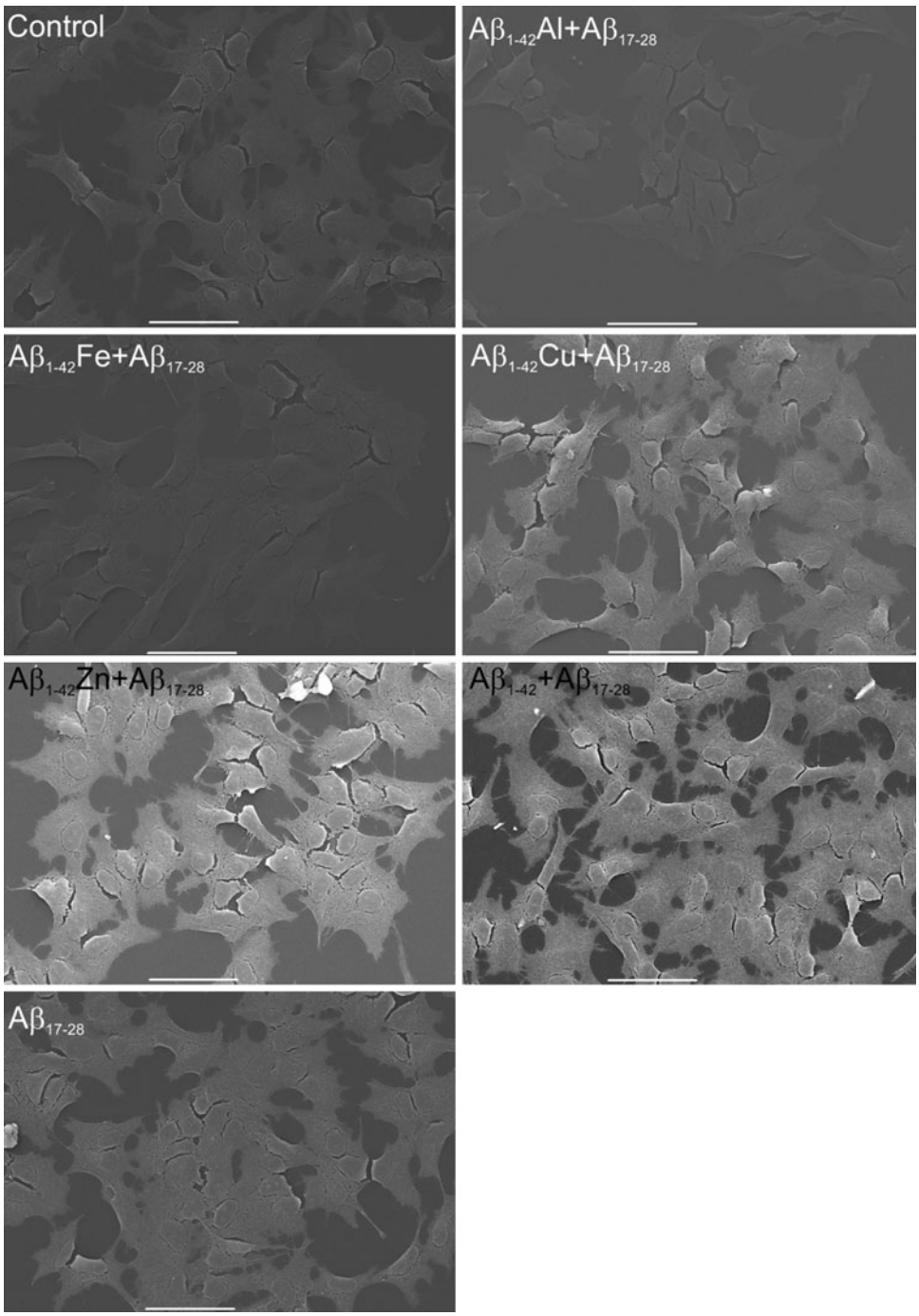

Fig. 3 SEM of neuroblastoma cells treated with the A$\beta_{1–42}$–metal complexes in the presence of A$\beta_{17–28}$ and with A$\beta_{17–28}$ alone after 24 h of incubation at room temperature

aggregational and toxic properties [24, 26, 27]. In spite of the fact that A$\beta_{17–28}$ is not physiologically relevant in AD, such a peptide is used as a case study for the specific purpose of emphasizing how hydrophobicity plays a crucial role in A$\beta_{1–42}$ toxicity; furthermore, this toxicity is increased when the peptide is complexed with metal ions, particularly Al^{3+}.

For both A$\beta_{1–42}$ [23] and A$\beta_{17–28}$, binding to Al resulted in an increase in superficial hydrophobicity and aggregation, as shown by ANS and ThT fluorescence measurements, respectively. In the presence of the A$\beta_{17–28}$–Al complex, the values of ThT fluorescence significantly increase with time (Fig. 1) compared with A$\beta_{17–28}$ alone and the other A$\beta_{17–28}$–metal complexes. In addition, it has been demonstrated that Al^{3+} has the ability to considerably enhance the exposure of the A$\beta_{17–28}$ hydrophobic cluster, as can be seen in Fig. 2. Also, the turbidity assay confirmed that Al greatly stimulates A$\beta_{17–28}$ aggregation; in fact, an increase in absorbance, as reported in Fig. 4, is due to the presence of an increased number of aggregates in solution.

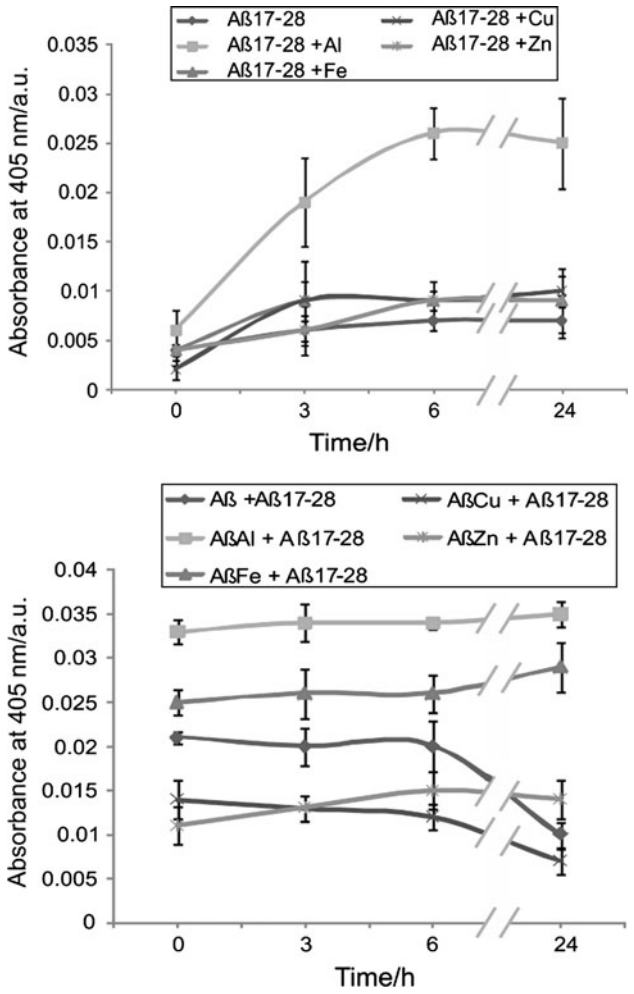

Fig. 4 Turbidity kinetic assay of $A\beta_{17–28}$ performed in both the absence and the presence of Al, Cu, Fe, and Zn at a concentration of 5 μM, and of $A\beta_{17–28}$ performed in the presence of $A\beta_{1–42}$–metal complexes. The $A\beta_{17–28}$, $A\beta_{1–42}$, and $A\beta_{1–42}$–metal complex peptide concentrations were 5 μM. Turbidity was measured at 405 nm. The data represented are the mean ± SD of three individual experiments. All readings were corrected for background absorbance

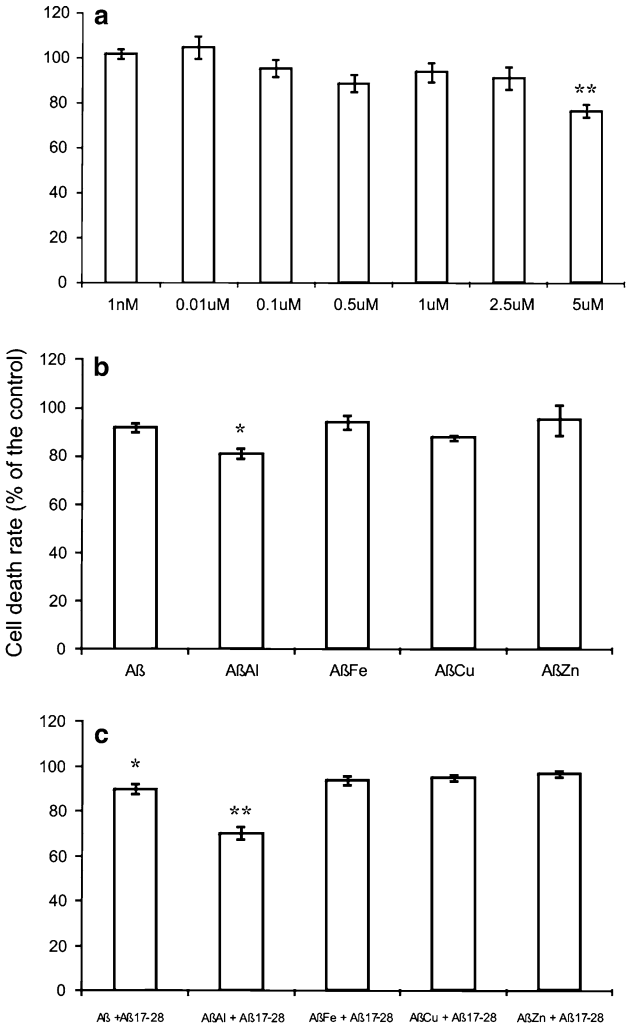

Fig. 5 Viability of human neuroblastoma cells measured by MTT assay. The dependence of neurotoxicity (% cell death as compared with control) on the concentration of $A\beta_{17–28}$ is shown (**a**). SH-SY5Y cells were incubated for 24 h with $A\beta_{1–42}$ alone, $A\beta_{1–42}$–metal complexes (peptide concentration = 0.5 μM), and with (**b**) or without (**c**) $A\beta_{17–28}$ (0.1 μM). The peptide mixture was allowed to incubate at room temperature for 24 h so that the peptides could interact before they were added to the cell medium. The data represented are the mean ± SD of three individual experiments, each done in triplicate. $^{**}P < 0.01$ versus control (chart B reprinted with permission from [23])

The peculiar structural conformation of the $A\beta_{1–42}$–Al complex resulted in significant toxicity to the SHSY5Y cell culture, as shown in Fig. 5b. This result, according to early studies on ThT dye [28], may seem contradictory because the nonfibrillar species should be more toxic than the fibrillar ones [4]. Recent investigations, however, have reported that ThT binds to Aβ protofibrils [15] but—surprisingly—also to soluble oligomers [14]. For these reasons, we can hypothesize that the increased fluorescence of ThT was due to the presence of a large amount of oligomeric species in solution, as also confirmed by TEM micrographs (Fig. 6).

After preliminary analysis of $A\beta_{17–28}$ in the presence of metal ions, the interaction between the truncated fragment and $A\beta_{1–42}$–metal complexes was studied. Our data suggest that $A\beta_{17–28}$ enhances $A\beta_{1–42}$–Al oligomerization, as is apparent from ThT fluorescence (Fig. 1c) [14] and TEM images (Fig. 6). $A\beta_{1–42}$–Al + $A\beta_{17–28}$ oligomers are characterized by the exposure of hydrophobic residues, as revealed by the marked increased in ANS fluorescence compared with the other $A\beta_{1–42}$–metal complexes.

Although Al is an exogenous metal ion, it has been demonstrated to possess the capacity to strongly influence Aβ conformational changes, especially when compared with endogenous biometals such as Fe, Cu, and Zn.

It is worth noting that $A\beta_{17–28}$ stimulates $A\beta_{1–42}$–metal complex (with Fe, Cu, and Zn) fibrillization rather than

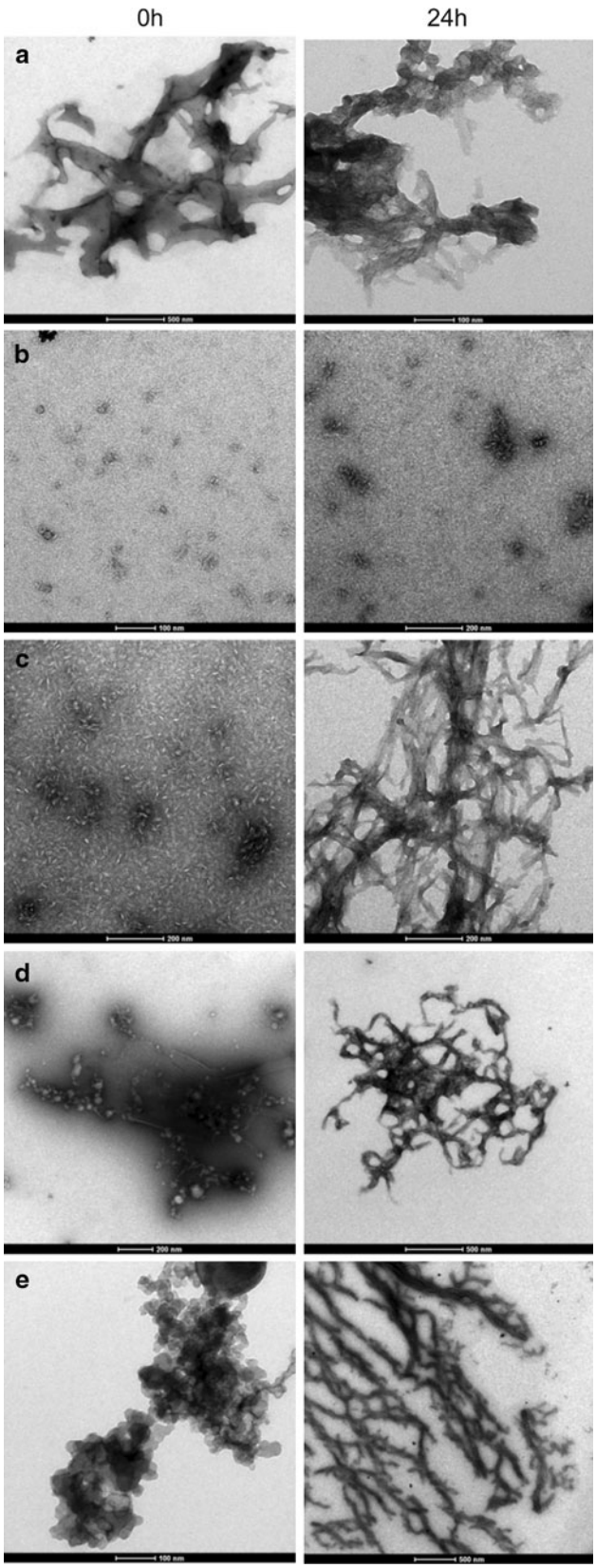

◀ **Fig. 6** TEM micrographs of $A\beta_{1-42}$ and $A\beta_{1-42}$–metal complexes in the presence of $A\beta_{17-28}$ at time 0 and after 24 h of incubation at room temperature. **a** $A\beta_{1-42}$ + $A\beta_{17-28}$, **b** $A\beta_{1-42}$–Al + $A\beta_{17-28}$, **c** $A\beta_{1-42}$–Cu + $A\beta_{17-28}$, **d** $A\beta_{1-42}$–Fe + $A\beta_{17-28}$, **e** $A\beta_{1-42}$–Zn + $A\beta_{17-28}$

oligomerization, in contrast to what was seen for $A\beta_{1-42}$–Al; this was primarily detected by electron microscopy. Accordingly, we should observe a dramatic increase in ThT fluorescence due to $A\beta_{1-42}$–metal ions + $A\beta_{17-28}$ aggregation. However, the increase of fluorescence was actually negligible. We can thus speculate that $A\beta_{1-42}$–metal complexes + $A\beta_{17-28}$ fibrils precipitated due to their high molecular weight and lipophilicity. In fact, we did not observe changes, even after mechanical stirring (data not shown).

Recent reports have highlighted the critical role played by $A\beta$ soluble oligomers [2, 29, 30]. Coherently, we observed a high cellular toxicity upon $A\beta_{1-42}$–Al + $A\beta_{17-28}$ treatment, with this treatment being the only complex that formed oligomers in our experimental condition, while in the presence of the other $A\beta_{1-42}$–metal complexes + $A\beta_{17-28}$ we observed mainly insoluble fibrillary structures. The toxicity of $A\beta_{1-42}$–Al + $A\beta_{17-28}$ is significant not only when compared to that of the control, but even more so when compared with that of $A\beta_{1-42}$–Al alone. It should be remembered that we initially used a nontoxic $A\beta_{17-28}$ concentration. It is possible to establish that the toxicity of $A\beta_{1-42}$–Al + $A\beta_{17-28}$ was due to the increased hydrophobicity that characterizes these models.

It is still not yet completely clear how $A\beta$ induces toxicity [31]. Nevertheless, several mechanisms of neurotoxicity have been proposed, such as a capacity to induce mitochondrial apoptotic pathways [32], pro-oxidant effects [33], and the ability to induce apoptosis through the activation of caspases [34]. Besides these complex apoptotic mechanisms, it has been proposed that $A\beta_{1-42}$ and its metal complexes (especially $A\beta_{1-42}$–Al) could interact significantly with cell lipid bilayers [20], perturbing membrane fluidity and thus their physiological properties, leading to a generalized increase in bilayer permeability which could induce cell death [35, 36]. Accordingly, it is not surprising that $A\beta_{1-42}$–Al produces the most relevant alteration; this is probably due to its elevated superficial hydrophobicity (as confirmed by ANS fluorescence) and its stable oligomeric structure (as confirmed by TEM). From these observations we can deduce that the enhanced toxicity induced by $A\beta_{1-42}$–Al + $A\beta_{17-28}$ is due to its increased superficial hydrophobicity, which could act as "shrapnel." In fact, our results highlight how the neurotoxicity is directly related to the $A\beta_{1-42}$–metal + $A\beta_{17-28}$ complex

superficial hydrophobicity (except for $A\beta_{1–42}$–Zn + $A\beta_{17–28}$, which has a propensity to precipitate). In our opinion, the surface hydrophobicity is key to understanding the toxicity of $A\beta_{1–42}$ for two reasons: first, because several reports highlight the role played by $A\beta$ in the disruption of membrane fluidity [20, 37]; second, we can assume that the exposure of hydrophobic clusters by $A\beta_{1–42}$ and by its metal complexes facilitates the interaction with the lipophilic cellular bilayer, bringing $A\beta_{1–42}$ oligomers from a higher to a lower protein energy state [38].

In conclusion, data reported herein underline the key role played by superficial hydrophobicity in modulating $A\beta_{1–42}$–metal complex toxicity. In particular, the MTT assay indicated that cellular toxicity can be enhanced in the presence of several metal ions, but the metals play different roles. In fact, different morphological structures can be observed with different $A\beta$–metal ion complexes, depending on the amino acid residues that coordinate the different metal ions [38]. Meanwhile, Al increases the formation of low-dimensional and highly hydrophobic aggregates (such as oligomers, as shown by TEM); the other metal ions favor the formation of large, amorphous aggregates. This paper has not focused only on the $A\beta_{1–42}$ aggregation pathway in the presence of metal ions; the main focus has been on the importance of superficial hydrophobicity as a crucial feature to discern whether different $A\beta_{1–42}$ species have a greater or lesser ability to cause neuronal toxicity. In our opinion, $A\beta_{1–42}$–metal + $A\beta_{17–28}$ neurotoxicity is not merely due to oxidative stress mechanisms mediated by the presence of metal ions; indeed, the toxicity of $A\beta_{1–42}$–Al + $A\beta_{17–28}$ is greater than those of both the control and $A\beta_{1–42}$–Al alone.

Materials and methods

Materials

Human β-amyloid 1–42 was purchased from Invitrogen. β-amyloid truncated fragment 17–28, thioflavin T (ThT), ANS, L-lactic acid aluminum salt, $FeCl_3$, $CuCl_2$, $ZnCl_2$, and 3-(4,5-dimethylthiazol-2-yl)-2,5-diphenyltetrazolium bromide (MTT) were purchased from Sigma-Aldrich (St. Louis, MO, USA). Experiments with $CuCl_2$ were carried out in PBS pH 7.4 buffer, while all other experiments were developed in 0.1 M Tris/HCl pH 7.4 buffer plus 0.15 M NaCl (standard medium).

Preparation of Aβ–metal complexes

Human $A\beta_{1–42}$ was dissolved in hexafluoroisopropanol (HFIP) for 40 min at room temperature and then separated into aliquots. HFIP was removed under vacuum in a Speed Vac (Sc110 Savant Instruments). This treatment was repeated three times (modified protocol from Dahlgren et al. [11]). $A\beta$ fragment 17–28 (1 mg) was dissolved in 2 cm^3 of HFIP for 3 h at room temperature and then separated into aliquots. The solvent was removed under vacuum as done for human $A\beta_{1–42}$; this treatment was repeated twice more with a latency period in HFIP of 40 min. The $A\beta_{1–42}$–metal complexes were prepared by 24 h of dialysis against 10 mM metal solutions ($[CH_3CH(OH)COO]_3Al$, $FeCl_3$, $CuCl_2$, $ZnCl_2$) at $T = 4$ °C using Spectra/Por® Float-A-Lyser® tubes (Spectrum Labs) with a molecular weight cut-off (MWCO) of 1000. Then, $A\beta_{1–42}$ metal complexes were dialyzed against distilled water (three water changes) for 24 h to remove the excess of metals. The same treatment was also performed with $A\beta$ alone [12]. Aliquots of $A\beta_{1–42}$, $A\beta_{1–42}$–metal complexes, and $A\beta_{17–28}$ were stored at −20 °C until used.

Fluorescence measurements

Fluorescence measurements were performed with a Perkin-Elmer LS 50B spectrofluorimeter equipped with a thermostatic cell holder and magnetic stirring. The experiments were carried out at 25 °C. Fluorescence tests with ThT (12 μM) were developed on solutions containing 5 μM $A\beta$ fragment 17–28 and the metal ions Al^{3+}, Fe^{3+}, Cu^{2+}, and Zn^{2+} (1:1 ratio), and on solutions containing 5 μM human $A\beta_{1–42}$ alone or complexed with Al^{3+}, Fe^{3+}, Cu^{2+}, and Zn^{2+} along with 5 μM $A\beta$ fragment 17–28. Development was followed for 24 h by monitoring the increase in the fluorescence intensity at 482 nm with excitation at 450 nm.

Turbidity measurements

Turbidity assays were performed in 300 mm^3 96-well plates (Falcon). The absorbance of all samples was measured at 405 nm using a Microplate SPECTRAmax®. The solutions were stirred for 25 s before reading to suspend the aggregates. The absorbance due to the buffer alone was subtracted from that of the buffer plus metal ions. Turbidity measurements were carried out to quantify the presence of aggregates due to the interaction between human $A\beta_{1–42}$ and its truncated fragment, and between $A\beta_{17–28}$ and metal ions (Al^{3+}, Fe^{3+}, Cu^{2+}, and Zn^{2+}).

Transmission electron microscopy

All samples at a protein concentration of 10 μM, and after an incubation period of 24 h, were absorbed onto glow-discharged carbon-coated Butwar films on 400-mesh copper grids. The grids were negatively stained with 1% uranyl acetate and observed at 40,000× by transmission electron microscopy (Tecnai G2, FEI). The samples observed

contained $A\beta_{1-42}$ and its metal complexes with $A\beta_{17-28}$ (1:1 ratio) or $A\beta_{17-28}$ in solution with Al^{3+}, Fe^{3+}, Cu^{2+}, and Zn^{2+} (concentration ratio 1:1).

Neuroblastoma cells

SH-SY5Y human neuroblastoma cells were purchased from the ECACC (European Collection of Cell Culture, Salisbury, UK). The medium in which they were cultured contained DMEM/F12 (Gibco, Carlsbad, CA, USA) with 15% (v/v) fetal bovine serum (FBS, Sigma-Aldrich, St. Louis, MO, USA), 100 units/cm^3 penicillin and 100 μg/cm^3 streptomycin (Gibco, Carlsbad, CA, USA) and 1% (v/v) MEM nonessential amino acid (NEAA) (Sigma-Aldrich, St. Louis, MO, USA). Cells were stored at 37 °C with 5% CO_2 in a humidified atmosphere (90% humidity). Cells were used until passage 35. The culture medium was replaced every 2 days.

Cell viability assay

Cell viability was determined through an MTT reduction assay. SH-SY5Y cells were seeded into 24-well plates at a density of 7×10^4 cells per well in 1 cm^3 culture medium. An FBS culture medium (2%) containing (1) $A\beta_{1-42}$, (2) $A\beta_{1-42}$–metal complexes with or without $A\beta_{17-28}$, (3) $A\beta_{17-28}$ with or without metals, or (4) metal ions alone (Al^{3+}, Fe^{3+}, Cu^{2+}, and Zn^{2+}) was added to the cells for 24 h. MTT (100 mm^3, 5 mg/cm^3) was added to each well and incubated in the dark at 37 °C for 3 h. After that, the cells were lysed with 1 cm^3 of acidic isopropanol (0.04 M HCl in absolute isopropanol) [13]. Color intensity was measured with a 96-well ELISA plate reader at 550 nm (Microplate SPECTRAmax®). All MTT assays were performed three times in triplicate. Viability was defined as the relative absorbance of the treated versus the untreated, expressed as a percentage.

Scanning electron microscopy of human neuroblastoma cells

SH-SY5Y cells were seeded onto glass cover slips and treated with $A\beta_{1-42}$ and $A\beta_{1-42}$–metal complexes with or without the interaction with $A\beta_{17-28}$. After 24 h of incubation, the cells on glass cover slips were fixed with formaldehyde pH 7.4 and dehydrated in a graded ethanol series. Then the samples were critical point dried with CO_2 in a HCP-2 Hitachi 2 Critical Point Dryer and gold-coated for examination under a JEDL JSM-6490 scanning electron microscope. The working pressure was 4.2–4.3 bar and the temperature was 5 °C. Untreated cells (control) were also examined for comparison.

Statistical analysis

MTT, turbidity, and ThT fluorescence assays were statistically analyzed by ANOVA followed by the Student–Newman–Keuls t test as a post hoc test. Results were reported to be highly statistically significant if $P < 0.01$ and statistically significant if $P < 0.05$. Results are presented as mean ± standard deviation.

Acknowledgment This work was supported by PRIN 2007.

References

1. Iqbal K, Liu F, Gong CX, Alonso AD, Grundke-Iqbal I (2009) Acta Neuropathol 118:53
2. Ono K, Condron MM, Teplow DB (2009) Proc Natl Acad Sci USA 106:14745
3. Savva GM, Wharton SB, Ince PG, Forster G, Matthews FE, Brayne C (2009) N Engl J Med 360:2302
4. Nygaard HB, Strittmatter SM (2009) AMA Arch Neurol 66:1325
5. Zatta P, Drago D, Bolognin S, Sensi SL (2009) Trends Pharmacol Sci 30:346
6. Lovell MA, Robertson JD, Teesdale WJ, Campbell JL, Markesbery WR (1998) J Neurol Sci 158:47
7. Miller LM, Wang Q, Telivala TP, Smith RJ, Lanzirotti A, Miklossy J (2006) J Struct Biol 155:30
8. Leskovjan AC, Lanzirotti A, Miller LM (2009) Neuroimage 47:1215
9. Zbilut JP, Webber CL, Colosimo A, Giuliani A (2000) Protein Eng 13:99
10. Kim W, Hecht MH (2006) Proc Natl Acad Sci USA 103:15824
11. Dahlgren KN, Manelli AM, Stine WB, Baker LK, Krafft GA, LaDu MJ (2002) J Biol Chem 277:32046
12. Drago D, Folin M, Baiguera S, Tognon G, Ricchelli F, Zatta P (2007) J Alzheimers Dis 11:33
13. Shearman MS, Hawtin SR, Tailor VJ (1995) J Neurochem 65:218
14. Maezawa I, Hong HS, Liu R, Wu CY, Cheng RH, Kung MP, Kung HF, Lam KS, Oddo S, LaFerla FM, Jin LW (2008) J Neurochem 104:457
15. Ferreira ST, Vieira MNN, De Felice FG (2007) IUBMB Life 59:332
16. Naiki H, Gejyo F, Nakakuki K (1997) Biochemistry 36:6243
17. Uversky VN, Winter S, Lober G (1996) Biophys Chem 60:79
18. Drago D, Bolognin S, Zatta P (2008) Curr Alzheimer Res 5:500
19. Friedman R, Pellarin R, Caflisch A (2009) J Mol Biol 387:407
20. Suwalsky M, Bolognin S, Zatta P (2009) J Alzheimers Dis 17:81
21. Yankner BA, Lu T (2009) J Biol Chem 284:4754
22. Kopito RR, Ron D (2000) Nat Cell Biol 2:E207
23. Drago D, Bettella M, Bolognin S, Cendron L, Scancar J, Milacic R, Ricchelli F, Casini A, Messori L, Tognon G, Zatta P (2008) Int J Biochem Cell B 40:731
24. Millucci L, Ghezzi L, Bernardini G, Santucci A (2010) Curr Protein Pep Sc 11:457
25. Atamna H (2009) J Bioenerg Biomembr 41:457
26. Tjernberg LO, Callaway DJE, Tjernberg A, Hahne S, Lilliehook C, Terenius L, Thyberg J, Nordstedt C (1999) J Biol Chem 274:12619
27. Melquiond A, Dong X, Mousseau N, Derreumaux P (2008) Curr Alzheimer Res 5:244
28. Levine H (1993) Protein Sci 2:404

29. Xue WF, Hellewell AL, Gosal WS, Homans SW, Hewitt EW, Radford SE (2009) J Biol Chem 284:34272
30. Zhang A, Qi W, Good TA, Fernandez EJ (2009) Biophys J 96:1091
31. Shah SB, Nolan R, Davis E, Stokin GB, Niesman I, Canto I, Glabe C, Goldstein LSB (2009) Neurobiol Dis 36:11
32. Deshpande A, Mina E, Glabe C, Busciglio J (2006) J Neurosci 26:6011
33. Behl C, Davis JB, Lesley R, Schubert D (1994) Cell 77:817
34. Nakagawa T, Zhu H, Morishima N, Li E, Xu J, Yankner BA, Yuan JY (2000) Nature 403:98
35. Kremer JJ, Pallitto MM, Sklansky DJ, Murphy RM (2000) Biochemistry 39:10309
36. Lashuel HA, Hartley D, Petre BM, Walz T, Lansbury PT (2002) Nature 418:291
37. Eckert GP, Wood WG, Muller WE (2005) Subcell Biochem 38:319
38. Miller Y, Ma B, Nussinov R (2010) Chem Rev 110:4820